universe

Article

Polaron Dynamics in a Quasi-Two-Dimensional Bose–Einstein Condensate

Shukhrat N. Mardonov [1,2,3,†], Bobir A. Toshmatov [2,4,5,†], Bobomurat J. Ahmedov [1,2,6,*,†] and Shukurillo T. Inoyatov [7,†]

1 Institute of Fundamental and Applied Research, "TIIAME" National Research University, Kori Niyozi 39, Tashkent 100000, Uzbekistan
2 Ulugh Beg Astronomical Institute, Astronomy St. 33, Tashkent 100052, Uzbekistan
3 Institute of Engineering Physics, Samarkand State University, University Ave. 5, Samarkand 140104, Uzbekistan
4 School of Mathematics and Natural Sciences, New Uzbekistan University, Mustaqillik Ave. 54, Tashkent 100007, Uzbekistan
5 Department of Physics and Chemistry, "TIIAME" National Research University, Kori Niyozi 39, Tashkent 100000, Uzbekistan
6 Physics Faculty, National University of Uzbekistan, Tashkent 100174, Uzbekistan
7 Department of Physics, Namangan State University, Uychi St. 316, Namangan 160136, Uzbekistan
* Correspondence: ahmedov@astrin.uz
† These authors contributed equally to this work.

Abstract: The concept of polaron quasiparticles was first introduced in the pioneering papers by Landau and Feynman in the 1930s and 1940s. It describes the phenomenon of an external particle producing a bound state in an embedded medium. Since then, the study of polaron quasiparticles has been an active area of research in condensed matter physics, with a wide range of applications in magnetic phenomena and lattice deformation properties. In this paper, we provide a comprehensive review of the polaron quasiparticle phenomenon, including its historical origins, theoretical developments, and current research. We also study the various applications of polaron quasiparticles in condensed matter physics, including in magnetic phenomena and lattice deformation properties. The review concludes with an outlook on future directions of research in this field. In particular, we study the motion of external embedded particles in a quasi-two-dimensional Bose–Einstein condensate confined by the quantum harmonic oscillator. We found that the dynamics of attracting particles with static Bose–Einstein condensate exhibit circular and precessional elliptic trajectories due to centripetal force. Polaron-forming embedded particles in the condensate lead to a strongly nonlinear trajectory of the polaron and dynamics of condensate depending on the initial parameters of the condensate and polaron.

Keywords: polarons; Bose–Einstein condensate; Gross–Pitaevskii equation

Citation: Mardonov, Sh.N.; Toshmatov, B.; Ahmedov, B.J.; Inoyatov, S.T.; Polaron Dynamics in a Quasi-Two-Dimensional Bose–Einstein Condensate. *Universe* **2023**, *9*, 89. https://doi.org/10.3390/universe9020089

Academic Editor: Tiberiu Harko

Received: 30 December 2022
Revised: 24 January 2023
Accepted: 5 February 2023
Published: 8 February 2023

1. Introduction

The concept of polaron quasiparticles was first introduced in the pioneering papers by Landau [1,2] and Feynman [3] in the 1930s and 1940s. It describes the phenomenon of an external particle producing a bound state in an embedded medium. This is a nonlinear physics phenomenon and is considered one of the most interesting and applicable in condensed matter theories. The polaron quasiparticles have a wide range of applications in condensed matter physics, including magnetic phenomena [4] and lattice deformation properties [5–7]. We first provide a comprehensive review of the polaron quasiparticle phenomenon, including its historical origins, theoretical developments, and current research.

The theoretical developments of polaron quasiparticles have been a subject of active research in recent years. The first theoretical description of polaron quasiparticles was given by Landau and Feynman, who introduced the concept of an external particle producing a bound state in an embedded medium. Since then, many researchers have contributed to the development of polaron quasiparticles theory. One of the most important contributions has been the development of the Fröhlich Hamiltonian, which describes the interaction between the external particle and the medium. This Hamiltonian has been used to study the properties of polaron quasiparticles, including the polaron effective mass and the polaron binding energy. Polaron quasiparticles have a wide range of applications in condensed matter physics. One of the most important applications is in magnetic phenomena, where polaron quasiparticles can be used to describe the behavior of electrons in magnetic materials. Another important application is in lattice deformation properties, where polaron quasiparticles can be used to describe the behavior of electrons in solids. In recent years, there has been a growing interest in the study of polaron quasiparticles in low-dimensional systems, including in graphene and other two-dimensional materials.

The buried particle is forced to interact with a comparatively soft medium (with a strong dependence on external forces) in order to generate a polaron quasiparticle. The formation of polaron states can be realized in a quantum soft medium as Bose–Einstein condensate (BEC). A massive bound state can be generated due to a change in density by effect of an external particle embedded in the condensate [8–11]. The induced modification can either be positive or negative depending on the nature of force (attraction or repulsion) between the external particle and condensate. Different regimes of the coupled motion of the condensate and the produced polaron can be induced by this variation. Apparently, the dynamics as a whole is significantly changed by the shift in the condensate's form. The Bose–Einstein condensate may be experimentally produced in a variety of dimensionalities by optical confinement [12–15] which indicates the importance of the condensate's dimension for the BEC polarons. The polaron states [16,17] can be produced in cold atomic Fermi gases [18,19]. Attractive and repulsive Fermi polarons are experimentally extracted in two dimensions [20]. The theory and nature of the polarons in the BEC are similar to some versions of the quantum field theory (see, e.g., [21–23]). The study of several regimes of the polaron properties [24–28] is based on the Gross–Pitaevskii equation (GPE) [8] for the Bose–Einstein condensate. The reasonable relation between the experimental observation of the dynamical process of the polaron and the condensate is found in the interesting article [29].

Polaron dynamics in one-dimensional BEC are strongly confined by two directions and demonstrate strong nonlinear oscillations along the coordinate [30] and unlike it, the two-dimensional system opens wide avenues for polaron dynamics [20].

In this study, we focus on the dynamics of an externally embedded particle in a two-dimensional BEC confined by parabolic potential, where interaction between particle and condensate is attractive rather than repulsive [31]. Additionally, we only consider non-self-interacting BEC to avoid the strong effect of repulsive interatomic interaction or collapse of condensate caused by attractive interatomic interaction [32–34]. We concentrate on the coupled nonlinear mechanics of the polaron and BEC confined in a parabolic potential, as determined by the GPE. Instead of considering the specific microscopic properties of the polaron, we focus on the coupled nonlinear mechanics of the polaron and BEC defined by the GPE.

Here, we assume that the embedded particle is significantly heavier with compare to the condensate particles, allowing us to view the embedded particle as a classical-like particle and the condensate as a quantum soft matter for the embedded particle, which can be characterized by a system of GPE and classical Newton equations [35,36]. This assumption enables us to analyze the dynamics of the system and understand the behavior of the particle and the condensate. Our main focus will be on particle dynamics with the static density profile and polarons formation with a nonuniform density of the condensate. Moreover, we assume that an embedded particle has an initial velocity v_0 perpendicular to the force that attracts the particle to the centre of mass of the condensate. The schematic form of the initial state of the system is presented in Figure 1. If the interaction between condensate and particle is considerably weak, then the condensate becomes a static potential for external particles leading to circular and precessional trajectories. If the interaction is relatively strong, such that the particle can modify the shape and shift the center of mass of the condensate from the origin of parabolic potential, then the condensate becomes a time-dependent potential for polaron-forming particles. As a result, the condensate deformation leads to highly nontrivial coupled dynamics of the particle and condensate. To interpret the dynamical properties, we will demonstrate the 2D trajectory of particles, the nontrivial interplay of the condensate position, angular momentum and forces for this strongly nonlinear system.

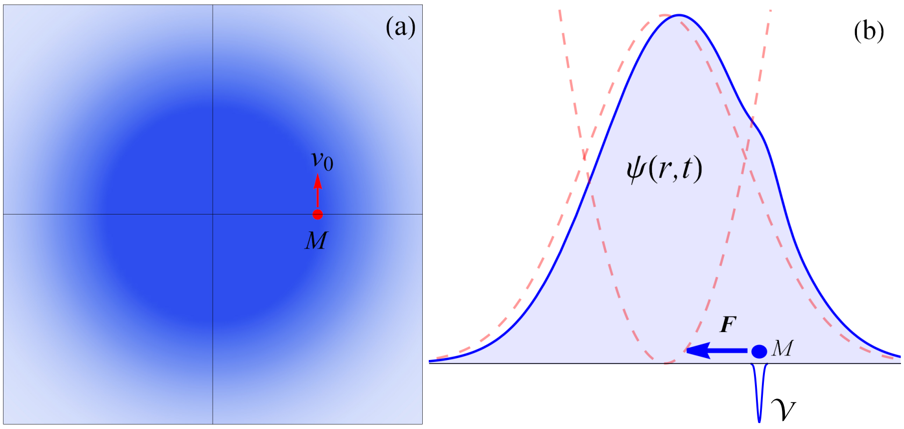

Figure 1. The schematic form of a model in two-dimensional (**a**) and one-dimensional cross-section (**b**) spaces. In panel (**a**) v_0 is the initial velocity of embedded particle M. In panel (**b**) $\psi(r,t)$ is characterising the BEC density profile, $\mathcal{V}$ is an attractive potential of embedded particles with mass M and the particle is located in some distance from the center of mass of the condensate. Red dashed lines present parabolic potential and static condensate profile, blue line presents a deformed condensate density profile for polaron-forming particles.

2. Model and Equations of the System

We consider a non-self-interacting quasi-two-dimensional BEC in a parabolic potential to model the system. The BEC is described by the Gross–Pitaevskii equation, which describes the time evolution of the condensate wavefunction. The embedded particle is treated as a point particle and its dynamics are described by Newton's equations of motion. The interaction between the BEC and the embedded particle is modelled by a potential that depends on the distance between the two.

In what follows, we set $\hbar \equiv \omega \equiv m \equiv 1$, with ω being frequency of parabolic potential and m being the condensate particle mass. We assume that the condensate wave function $\psi(\mathbf{r},t)$ ($\mathbf{r} = (x,y)$) is normalized by $2\pi \int_0^\infty |\psi(\mathbf{r},t)|^2 r dr = N$, with $N \gg 1$ being the total number of atomic particles in the condensate. Below we rescale the wave function by a factor $1/\sqrt{N}$ and use the GPE in the form:

$$i\frac{\partial}{\partial t}\psi(\mathbf{r},t) = \left(-\frac{1}{2}\nabla^2 + \frac{r^2}{2}\right)\psi(\mathbf{r},t) + \mathcal{V}(\mathbf{r} - \mathbf{R}(t))\psi(\mathbf{r},t). \tag{1}$$

Here $\mathcal{V}(\mathbf{r} - \mathbf{R}(t)) = V_0 \exp\left(-(\mathbf{r} - \mathbf{R}(t))^2/2\delta^2\right)$ describes the time-dependent potential of the particle locally interacting with condensate, where $\mathbf{R}(t) = (X(t), Y(t))$ determines trajectory of particle in plane (x,y). The amplitude is represented by a negative value, $V_0 < 0$, because the particle has an attractive interaction with the condensate, and the width $\delta \ll 1$ is much less than the condensate extension.

Since the mass of the condensate particle is equal to one then the total mass of the condensate is equal to a number of condensate particles N. We take into consideration an embedded particle with a mass equal to the mass of the condensate, that is $M = 1$ in the chosen units. It indicates that the embedded particle is substantially heavier than the atoms forming the condensate, therefore the trajectory of the embedded particle is defined by the classical Newton's equation:

$$M\ddot{\mathbf{R}}(t) = \mathbf{F}(\mathbf{R}(t))\,, \tag{2}$$

where $\mathbf{F}(\mathbf{R}(t))$ is the time-dependent force between condensate and external particle and it is defined as Ref. [37]

$$\mathbf{F}(\mathbf{R}(t)) \equiv -\partial_{\mathbf{R}(t)} \int_{-\infty}^{\infty} \mathcal{V}(\mathbf{r} - \mathbf{R}(t))|\psi(\mathbf{r}, t)|^2 d^2 r\,. \tag{3}$$

In order to characterize and describe all dynamics of the polaron-forming particles and the condensate, we use the system of Equations (1)–(3) [35,36]. From Equation (3) one can easily notice that the dynamics of polaron-forming embedded particles entirely depend on the dynamics of the wave function of the condensate, $\psi(\mathbf{r}, t)$. The center of mass of the condensate is an important dynamic parameter which is determined by the mean values of (x, y) as:

$$\begin{aligned} \langle x(t)\rangle &= \int_{-\infty}^{\infty} x|\psi(\mathbf{r}, t)|^2 d^2 r, \\ \langle y(t)\rangle &= \int_{-\infty}^{\infty} y|\psi(\mathbf{r}, t)|^2 d^2 r. \end{aligned} \tag{4}$$

Thus, the center of mass of the condensate is located at the point with coordinates $\langle \mathbf{r}(t)\rangle = (\langle x(t)\rangle, \langle y(t)\rangle)$.

For qualitative analysis, one can find the interaction energy between the particle and the condensate in a very narrow potential of the embedded particles ($\delta \ll 1$) compared to the expansion of the condensate as

$$V(\mathbf{R}(t)) = V_0 \int_{-\infty}^{\infty} |\psi(\mathbf{r}, t)|^2 \exp\left(-\frac{(\mathbf{r} - \mathbf{R}(t))^2}{2\delta^2}\right) d^2 r \approx 2\pi\tilde{V}|\psi(\mathbf{R}(t))|^2, \tag{5}$$

where $\tilde{V} \equiv V_0\delta^2$. In this approximation the force Equation (3) is determined by the gradient of (5) as

$$\mathbf{F}(\mathbf{R}(t)) = -\frac{\partial V(\mathbf{R}(t))}{\partial \mathbf{R}(t)} \equiv -2\pi\tilde{V}\frac{\partial|\psi(\mathbf{R}(t))|^2}{\partial \mathbf{R}(t)}. \tag{6}$$

A solution of the GPE (Equation (1)), which describes the dynamics of the BEC, can be represented in terms of the eigenfunctions of the parabolic potential, given by Equation (A1). These eigenfunctions provide a complete set of basis functions that can be used to express the wave function of the BEC, $\psi(\mathbf{r}, t)$, in terms of the eigenfunctions of the parabolic potential.

To demonstrate the system parameters and study the dynamics of the polaron-forming particle in the BEC, we solve the system of equations Equations (A3) and (A4) numerically. The set of initial conditions for the system, $\{A_{k_1', k_2}(0)\}$, is determined by minimizing the energy (Equation (A5)) for a given initial position $\mathbf{R}(0)$ of the embedded particle. This approach allows us to study the behavior of the polaron-forming particle in the BEC under a wide range of conditions and to explore how the confinement of the BEC by the parabolic potential affects its dynamics.

3. Particle Dynamics in a Static BEC

To understand the dynamics of external particles in the condensate, we begin by considering the condition of a static BEC. This means that the condensate is in a state of equilibrium and is not undergoing any time-dependent changes. By starting with this condition, we can better understand the behavior of the external particles in the presence of the condensate, and how their dynamics change as the condensate is perturbed or excited. This approach allows us to isolate the effect of the condensate on the external particles, and to study their behavior in a controlled and well-defined system.

We assume that the interaction between condensate and particle is weak ($\tilde{V} \ll 1$) and the condensate is always at rest [38]. This assumption leads us to neglect the last term of the GPE (1). Hence the energy of condensate (A5) occupies the lowest level of the harmonic oscillator with $n = 0$.

Consequently, the wave function (A2) of the condensate takes the following form:

$$\psi(\mathbf{r}, t) = \frac{1}{\sqrt{\pi}} \exp\left(-\frac{r^2}{2a^2}\right) \exp(-i\mu t)\,, \tag{7}$$

where $a = \sqrt{\hbar/m\omega} \equiv 1$ is the condensate extension, μ is the chemical potential of the condensate. As a result, the dynamics of the particle will be governed only by the solution of the Equation (2). By using the interaction energy approximation (5) with wave function (7) we rewrite Equation (2) in the form

$$M\ddot{\mathbf{R}}(t) = -2\pi\tilde{V}\frac{\partial|\psi(\mathbf{R}(t))|^2}{\partial\mathbf{R}(t)} \equiv 4\tilde{V}\mathbf{R}(t)\exp\left(-R^2(t)\right), \tag{8}$$

where $\dot{\mathbf{R}}(t) = \mathbf{v}(t) \equiv (v_x(t), v_y(t))$ stands for the velocity of the particle. The solution of the non-linear Equation (8) presents the complete picture of the particle trajectory in a static BEC.

Since the potential Equation (5) describes attraction between the particle and condensate, Equation (6) can provide the centripetal force for the particle. From this, it follows that for any initial velocity $\mathbf{v}(0)$ perpendicular to the vector $\mathbf{R}(0)$ the equation of the circular trajectory of the particle is defined by

$$M\frac{v_0^2}{R_0} = F(R_0), \tag{9}$$

where $v_0 \equiv |\mathbf{v}(0)|$ and $R_0 \equiv |\mathbf{R}(0)|$. Actually, due to the circular trajectory we have $v(t) \equiv v_0 = \text{const}$ and $R(t) \equiv R_0 = \text{const}$. Now by substituting Equations (6) and (7) to the Equation (9) we derive an equation

$$Mv_0^2 = 4|\tilde{V}|R_0^2\exp\left(-R_0^2\right). \tag{10}$$

As a result, Equation (10) determines the circular trajectory of the particle in a static BEC. Now we assume that the given initial velocity, $\mathbf{v}(0)$, and position, $\mathbf{R}(0)$, don't satisfy Equation (10). In this case, if $Mv_0^2 < 4|\tilde{V}|R_0^2\exp(-R_0^2)$, then the trajectory of the particle demonstrates quasi-apsidal-precession inside the circular orbit or if $Mv_0^2 > 4|\tilde{V}|R_0^2\exp(-R_0^2)$, then the trajectory of the particle demonstrates quasi-apsidal-precession outside the circular orbit. Figure 2 is presenting three particle trajectories: circular, elliptic precession outside the circle, and elliptic precession inside the circle of which each corresponds to a different initial velocity. In Figure 2a one can see that the red dashed trajectory makes more than full rotation at one circular rotation time t_0 of the particle even though the initial velocity decreased to $0.5v_0$. Correspondingly, blue dotted trajectory cannot make a full rotation even though its velocity is increased to $1.1v_0$. Furthermore, from Equation (8) it follows that the velocity of particle $\mathbf{v}(0)$ with circular trajectory strongly depends on interaction parameter $\tilde{V}$.

When the value of the interaction parameter, denoted as $\tilde{V}$, is increased, it can have the effect of compensating for the precession trajectory of a particle. In other words, if the precession of the particle's trajectory is an undesired effect, increasing the value of $\tilde{V}$ can help to counterbalance it. This can be useful in situations where the precession of the particle's trajectory is causing problems or disrupting the desired behavior. By adjusting the value of $\tilde{V}$, it is possible to exert more control over the motion of the particle and bring it closer to the desired trajectory.

From these results, we conclude that the condensate density distribution can change the trajectory of particles. On the right panel of Figure 2, we present long-time trajectories that correspond to the return time of the particle at the initial position. Figure 2 is plotted from the numerical solution of the system of Equations (A3) and (A4).

When a particle has a relatively high velocity $\mathbf{v}(0)$ at its initial point, it can fly out of the condensate. This is because the extension or size of the condensate is limited and cannot accommodate the high velocity of the particle. In other words, the condensate may not be able to contain the particle as it moves too quickly and exceeds the boundaries of the condensate. This is an important consideration to keep in mind when studying the behavior of particles within a condensate.

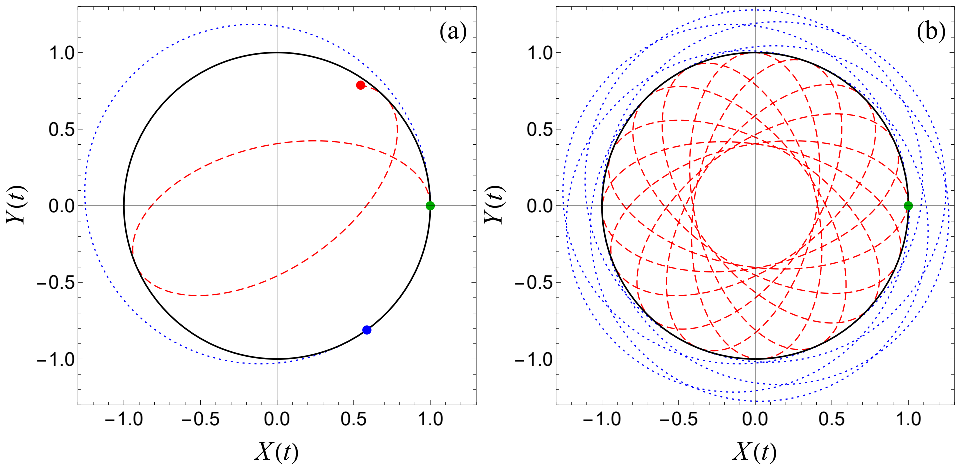

Figure 2. Plot of an embedded particle trajectory in a plane (x, y) for a static BEC. Initial parameters given by $M = 1$, $\mathbf{R}(0) = (1, 0)$, $\tilde{V} = -10^{-2}$. The lines correspond to different initial velocities given as $\mathbf{v}(0) = (0, 0.5v_0)$—red dashed, $\mathbf{v}(0) = (0, v_0)$—black solid and $\mathbf{v}(0) = (0, 1.1v_0)$ -blue dotted. Here, $v_0 = 2\big(|\tilde{V}|R_0^2 \exp(-R_0^2)\big)^{1/2} \approx 0.121$ is a circular orbit velocity, and a rotation period of a particle with a circular orbit is $t_0 = 2\pi R_0/v_0 \approx 51.8$. In plot (**a**) the trajectories correspond to the time t_0 and in plot (**b**) the trajectories correspond to the time t_f when the particle return to the initial position (blue point) $\mathbf{R}(t_f) \approx \mathbf{R}(0)$.

4. Polaron-Forming Particle and Condensate Dynamics

Here, we focus on the study of a specific type of external particle, known as a polaron-forming particle, in a BEC confined by a parabolic potential. A polaron-forming particle is a type of quasiparticle that forms when an external particle interacts with a medium in a nonlinear manner, creating a bound state. In this case, the medium is a BEC, and the external particle is the polaron-forming particle. The parabolic potential is used to confine the BEC, which allows for better control and manipulation of the system. By studying the behavior of the polaron-forming particle in this specific type of system, we can gain a deeper understanding of how polaron quasiparticles form and interact with their surrounding medium. Additionally, we can explore how the confinement of the BEC by parabolic potential modifies the properties of the polaron-forming particle.

We assume that initially an embedded particle in some coordinate leads to the deformation of density and displacement of the center of mass of the condensate. This static state of condensate can be obtained by increasing the interaction parameter between the particle and condensate. In a Figure 3 presented a ground state of quasi-two-dimensional condensate numerically obtained by minimization of the energy (A5) [39]. In the figure, black and grey points are the initial position of the embedded particle and condensate center of mass, correspondingly. From the figure, one can see that, the value of interaction parameter $\tilde{V} = -0.1$ is already enough to provide deformed nonuniform condensate density with a considerable displacement of the center of mass.

The trajectory of a rotating particle is heavily influenced by the various dynamical parameters that define the condensate. These dynamical parameters can include things such as the temperature, density, and overall structural characteristics of the condensate. They can also include the properties of the particle itself, such as its mass, charge, and velocity. The trajectory of the rotating particle is determined by the interplay between these different parameters, which can lead to complex and varied behaviors. As these parameters change, the trajectory of the particle will also change, and it can have a significant impact on the overall dynamics of the system.

It is important to take into account the influence of these dynamical parameters when trying to understand and predict the behavior of a rotating particle within a condensate. As these parameters are precisely controlled, the behavior of the particle can be studied in a controlled manner. In summary, the trajectory of a rotating particle is closely linked to the dynamical parameters of the condensate. These parameters play a crucial role in determining the particle's motion and understanding how they interact is essential to gain insight into the system.

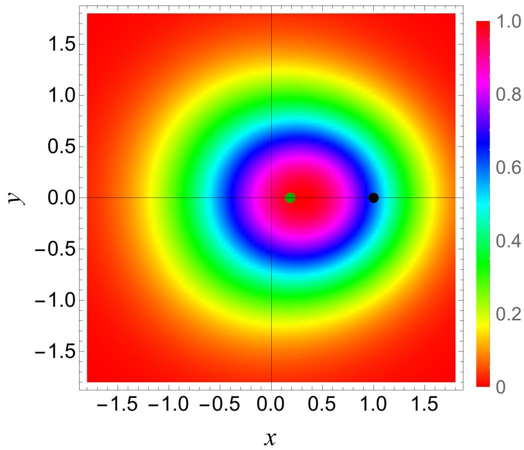

Figure 3. Ground state deformation of two-dimensional BEC density for initial parameters: $M = 1$, $\mathbf{R}(0) = (1, 0)$, $\tilde{V} = -10^{-1}$. Here the condensate center of mass is displaced at point $(\langle x(0)\rangle, \langle y(0)\rangle) \approx (0.184, 0)$ that fixed with gray point in the plot. The black point corresponds to the initial position of the polaron.

To demonstrate the effect of the polaron, besides its trajectory, we consider a projection of parallel and perpendicular unit vectors to interaction force (3) defined by

$$F_{\parallel}(t) = \mathbf{F}(\mathbf{R}(t)) \cdot \mathbf{n}_{\parallel}(t), \quad F_{\perp}(t) = \mathbf{F}(\mathbf{R}(t)) \times \mathbf{n}_{\parallel}(t). \tag{11}$$

Here "$\cdot$" - scalar and "$\times$" - cross product of vectors, $\mathbf{n}_{\parallel} = \mathbf{R}(t)/R(t)$. Moreover, we consider the angular momentum of the rotating polaron defined by

$$L_z(t) = M|\mathbf{R}(t) \times \mathbf{v}(t)|, \tag{12}$$

From Equations (11) and (12) we have following relation with the polaron formation:

$$\begin{aligned} &\text{if } F_{\perp}(t) = 0 \text{ and } L_z = \text{const} \leftrightarrow \text{ no polaron}, \\ &\text{if } F_{\perp}(t) \neq 0 \text{ and } L_z \neq \text{const} \leftrightarrow \text{ polaron}. \end{aligned} \tag{13}$$

From Equation (9) it follows that, for circular trajectory of particle $F_{\parallel}(t) = \text{const}$, $L_z(t) = \text{const}$ and $F_{\perp}(t) = 0$. Note that the total angular momentum of the system (BEC together with embedded particle) is conserved.

Figure 4 demonstrates the trajectory of the polaron, center of mass of the condensate Initial velocities of polaron v_0 defined by Equation (10) for corresponding interaction parameter $\tilde{V} = -0.1$ that has to provide circular trajectory without polaron effect. Comparing the Figure 4a,c with black solid and red dashed lines of Figure 2b correspondingly, we see the polaronic effect on the trajectories. In fact, these perturbations of polaron trajectories strongly being interconnected with the irregular dynamics of the center of mass of the condensate in Figure 4b,d. These interconnected nonuniform dynamics between the center of mass of condensate and polaron arise from the following causes:

(i), due to the polaron formation, the center of mass of ground state condensate is displaced at $\langle \mathbf{r}(0) \rangle$ that shown with the green point in Figures 3 and 4b,c;

(ii), when the polaron starts motion with a given initial velocity, the condensate center of mass follows the polaron due to attractive interaction. It follows that the center of mass becomes a function of the state of the polaron as $\langle \mathbf{r}(\mathbf{R}(t)) \rangle$. On the other hand $\langle \mathbf{r}(\mathbf{R}(t)) \rangle$ is the origin of the centripetal force (3) of $\mathbf{R}(t)$;

(iii), the parabolic potential confining the condensate induces an additional centripetal force for $\langle \mathbf{r}(\mathbf{R}(t)) \rangle$ defined by

$$\mathbf{F}_c(t) = -\frac{1}{2}\partial_{\langle \mathbf{r}(\mathbf{R}(t)) \rangle} \int_{-\infty}^{\infty} r^2 |\psi(\mathbf{r} - \langle \mathbf{r}(\mathbf{R}(t)) \rangle, t)|^2 d^2r = -\langle \mathbf{r}(\mathbf{R}(t)) \rangle, \tag{14}$$

where it is assumed that $\psi(\mathbf{r} - \langle \mathbf{r}(\mathbf{R}(t)) \rangle, t)$ is approximate ground state for polaron position $\langle \mathbf{r}(\mathbf{R}(t)) \rangle$. As a result, the polaron velocity $\mathbf{v}_t$ cannot resist the non-linearity between the centripetal forces (14) attracting the condensate to the origin of the coordinate and (3) attracting the polaron to the center of mass of the condensate. Eventually there arise strong irregularities to the trajectories, presented in Figure 4a,b. Moreover, decreasing initial velocity v_0 by factor 0.5 increases these irregular dynamics that correspond to Figure 4c,d. In Figure 4 red points present the final position of the particle and center of mass of the condensate. Figure 5a,b is a plot of parameters (11) and (12) that compare the cases of the static BEC with particle and displaced condensate with polaron. From the plots, it follows that polaron formation leads to strongly nonlinear oscillation of forces (11) and angular momentum (12). Furthermore, comparing to Figure 5a,b, one can see that decreasing of initial velocity v_0 increases the intensity of nonlinearity. Furthermore, Figure 5 completely proves the conditions (13).

Since Equation (8) is correct only for static condensate, the trajectory of the polaron and center of mass of the condensate cannot be in an equilibrium state. Figure 4 demonstrates the nonuniform trajectory of the particle and irregular center of mass of the condensate due to condensate dynamics caused by the polaron effect.

In order to determine the quasi-equilibrium dynamics of the condensate and polaron, we assume that the approximate function of the ground state for the system is represented by $\psi(\mathbf{r} - \langle \mathbf{r}(0) \rangle, 0)$. By using this assumption, we can calculate the new centripetal force experienced by the polaron with an origin located at $\langle \mathbf{r}(0) \rangle$ and from Equation (9) we derive

$$M\frac{v_0^2}{R_0} = F(R_0 - \langle r_0 \rangle) \approx F(R_0) - \langle r_0 \rangle \frac{\partial F(R_0)}{\partial R_0}. \tag{15}$$

The Equation (15) determines a small correction for initial velocity $\mathbf{v}(0)$ to find quasi-equilibrium dynamics between polaron and condensate, which is presented in Figure 6. From Figure 6a,b, one can see the trajectories of polaron and center of mass of the condensate presenting regular precession providing inner and outer circles. The distance between the inner and outer circles of Figure 6a is of the order of $\langle r_0 \rangle$. One of the important dynamic parameters of the BEC is a width [40] defined by

$$w(t) = \int_{-\infty}^{\infty} (\mathbf{r} - \langle \mathbf{r}(t) \rangle)^2 |\psi(\mathbf{r}, t)|^2 d^2r. \tag{16}$$

Comparing all dynamic parameters of Figure 6c and the condensate width (d) one can conclude all parameters oscillate with the same frequency on average that corresponds to the precession frequency of $\langle \mathbf{r}(t) \rangle$. The small irregular oscillations observed in the plots (c) are caused by the deformation in the condensate density, which can be characterized by analyzing the condensate width plot (d).

All demonstrated figures are given from the numerical solution of a system of Equations (A3) and (A4).

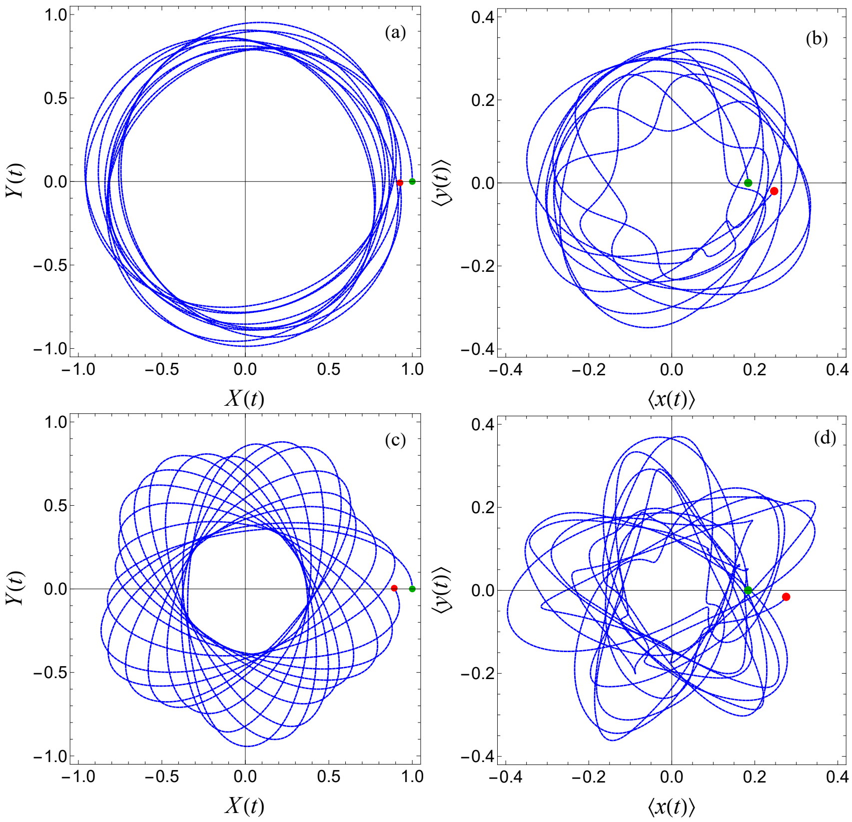

Figure 4. Plots of the polaron trajectories (**a**,**c**) and center of mass of the condensate (**b**,**d**) in a plane (x, y). Initial parameters are given in the caption of Figure 3. The plots (**a**,**b**) correspond to $\mathbf{v}(0) = (0, v_0)$ and (**c**,**d**) correspond to $\mathbf{v}(0) = (0, 0.5v_0)$ initial velocities. Corresponding circular orbit velocity for polaron is $v_0 = \left(4|\tilde{V}|R_0^2 \exp\left(-R_0^2\right)\right)^{1/2} \approx 0.384$. Plot times for (**a**,**b**) is $t_f = 133$ and for (**c**,**d**) is $t_f = 187.7$ which is taken thus the $\mathbf{R}(t_f)$—red point becomes close to $\mathbf{R}(0)$—initial blue point.

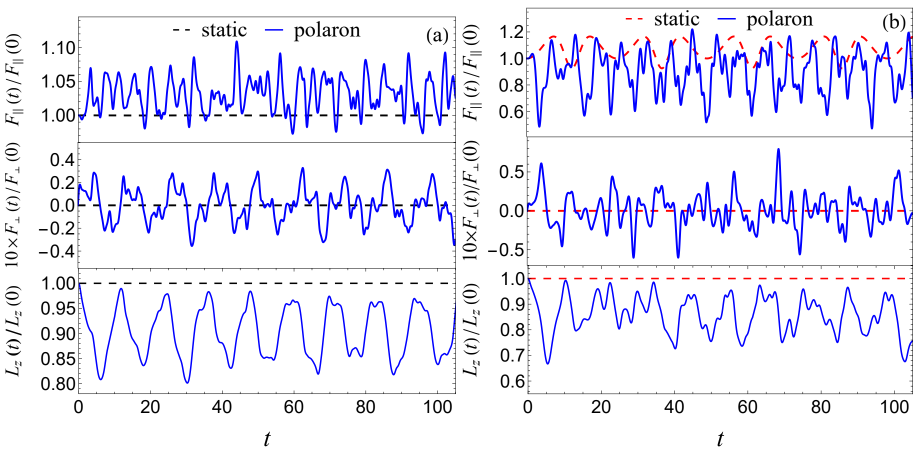

Figure 5. Plots of the parameters defined by Equations (6) and (12) for the initial velocities $\mathbf{v}(0) = (0, v_0)$ (**a**) and $\mathbf{v}(0) = (0, 0.5v_0)$ (**b**), correspondingly. All initial parameters are given in the caption of Figure 3.

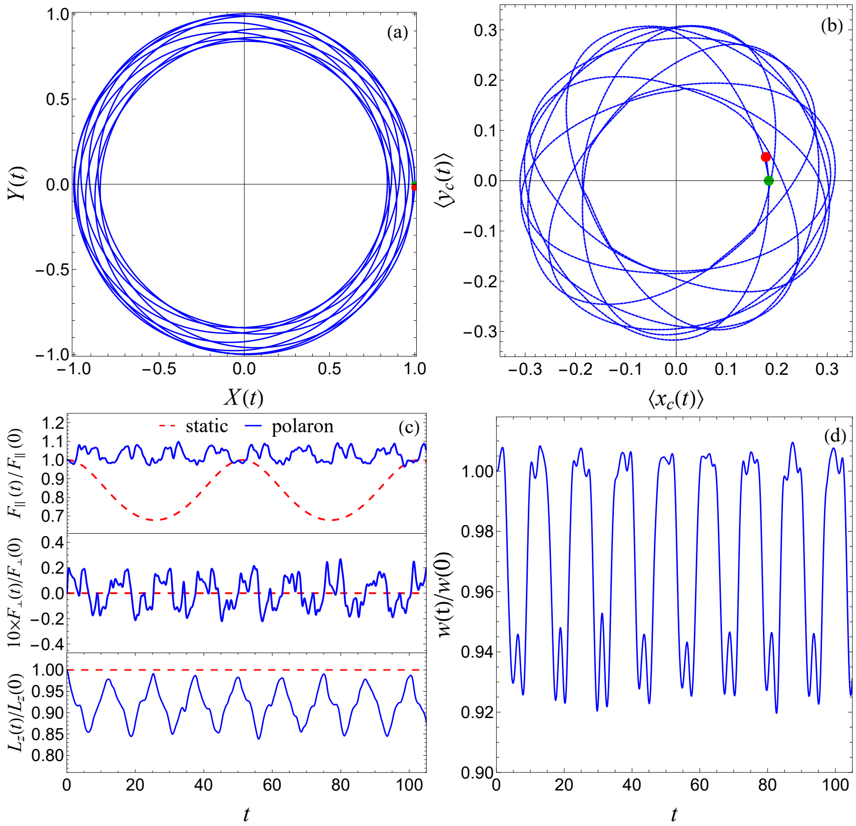

Figure 6. Plots of a polaron trajectory (**a**), the center of mass of the condensate (**b**), parameters (**c**) defined by Equations (11) and (12) and normalized condensate width (**d**). Here initial velocity of the polaron is defined by Equation (15) as $\mathbf{v}(0) = (0, 1.1v_0)$. All other initial parameters are the same with ground state Figure 3.

5. Conclusions

In this paper, we have provided a comprehensive review of the polaron quasiparticle phenomenon, including its historical origins, theoretical developments, and current research. We also discussed the various applications of polaron quasiparticles in condensed matter physics, including in magnetic phenomena and lattice deformation properties. The polaron quasiparticles are considered one of the most interesting and applicable in condensed matter theories, and the study of polaron quasiparticles will continue to be intriguing.

We studied the nonlinear dynamics of the embedded particle in a two-dimensional BEC confined by parabolic potential. We considered particle dynamics in a static BEC and polaron dynamics in a deformed density of the BEC. We have shown that in the case of weak interaction of the condensate with the particle, the condensate becomes a static potential for the particle, leading to circular and quasi-periodic trajectories of the particle.

To study the behavior of the BEC and the embedded particle, we performed numerical simulations of the system. We considered different initial conditions for the BEC and the embedded particle and studied the effects of the interaction on the BEC. We also investigated the role of the parabolic potential on the dynamics of the system. Our results show that the BEC and the embedded particle can exhibit a range of behaviors depending on the initial conditions and the strength of the interaction. In particular, we found that the parabolic potential can greatly affect the dynamics of the system and can lead to the formation of bound states between the BEC and the embedded particle.

If the interaction is relatively strong that can modify the density distribution and shift the center of mass of the condensate from the origin of parabolic potential, then condensate becomes a time-dependent potential for polaron-forming particles. As a result, a shift of the center of mass of the condensate produces a small correction to the particle velocity and the non-static center of mass leads to highly nontrivial coupled dynamics of the particle and condensate. Deformation of condensate density leads to the non-conservation of angular momentum of the polaron.

We have studied the interaction of a non-self-interacting quasi-two-dimensional BEC in a parabolic potential with an externally embedded particle. We have analyzed the behavior of the BEC and the embedded particle under different conditions and studied the effects of the interaction on the BEC. We also investigated the role of the parabolic potential on the dynamics of the system. Our results have important implications for the understanding of BECs and the behavior of particles embedded in them. In particular, our results suggest that the parabolic potential can greatly affect the dynamics of the system and can lead to the formation of bound states between the BEC and the embedded particle. Future work could include the study of the system with different types of interactions, different potentials, or in different dimensions.

Author Contributions: Conceptualization, S.N.M., B.A.T. and B.J.A.; methodology, S.N.M., B.J.A., B.A.T. and S.T.I.; software, S.N.M.; validation, B.J.A., B.A.T. and S.N.M.; formal analysis, B.J.A.; investigation, S.N.M. and B.A.T.; resources, S.N.M.; data curation, S.N.M.; writing—original draft preparation, S.N.M.; writing—review and editing, B.A.T. and B.J.A.; visualization, S.N.M.; supervision, S.N.M.; project administration, B.J.A.; funding acquisition, B.J.A. and S.T.I. All authors have read and agreed to the published version of the manuscript.

Funding: This research received no external funding.

Institutional Review Board Statement: Not applicable.

Informed Consent Statement: Not applicable.

Data Availability Statement: No data are available.

Acknowledgments: This research is supported by Grant of the Ministry for Innovative Development of Uzbekistan. The authors are grateful to E.Ya. Sherman for the valuable discussions.

Conflicts of Interest: The authors declare no conflict of interest.

Abbreviations

The following abbreviations are used in this manuscript:

BEC	Bose–Einstein condensate
GPE	Gross–Pitaevskii equation

Appendix A. Expansion in the Harmonic Oscillator Basis

In one-dimensional systems eigenfunctions of the parabolic potential is defined by

$$\psi_k(z) = \frac{H_k(z)}{\pi^{1/4}(2^k k!)^{1/2}} \exp\left(-\frac{z^2}{2}\right), \tag{A1}$$

with $H_k(x)$ being the corresponding Hermite polynomial [30]. This implies the expansion of the two-dimensional BEC wave function in the truncated basis [1], which is defined as follows:

$$\psi(x, y, t) = \sum_{k_1=0}^{n} \sum_{k_2=0}^{k_1} A_{k_1-k_2,k_2}(t)\psi_{k_1-k_2}(x)\psi_{k_2}(y), \tag{A2}$$

where $n+1$ $(n = 0, 1, 2, ...)$ determine energy levels of the parabolic potential in the plane (x, y), that have relation with indexes are $n = k_1 + k_2$. In Equation (A2) the total number of eigenfunctions is defined by $N = \sum_{i=1}^{n+1} i$ and the time-dependent coefficients normalized by $\sum_{k_1=0}^{n} \sum_{k_2=0}^{k_1} \left|A_{k_1-k_2,k_2}(t)\right|^2 = 1$. Below for simplicity we omit explicit $t-$dependencies and introduce the notations $k_1' \equiv k_1 - k_2$, $\sum_{\{k_1,k_2\}} \equiv \sum_{k_1=0}^{n} \sum_{k_2=0}^{k_1}$.

The time-dependent coefficients of wave function Equation (A2) one can find by integrating Equation (1)'s overall coordinate by multiplying both sides with a two-dimensional basis of the harmonic oscillator eigenstates as:

$$\begin{aligned} i\frac{\partial A_{k_1',k_2}}{\partial t} &= A_{k_1',k_2}(k_1+1)+ \\ &+ \sum_{\{k_3,k_4\}} A_{k_3',k_4}\int_{-\infty}^{\infty}\psi_{k_1'}(x)\psi_{k_2}(y)\mathcal{V}(x-X(t),y-Y(t))\psi_{k_3'}(x)\psi_{k_4}(y)dxdy, \end{aligned} \tag{A3}$$

where $k_3' = k_3 - k_4$.

In the two-dimensional system a velocity is a vector (v_x, v_y), that components are determined by $v_x(t) \equiv dX(t)/dt$ and $v_y(t) \equiv dY(t)/dt$. Therefore Equation (2) can be represented in a system of equations

$$\begin{aligned} &M\frac{dv_x(t)}{dt} = \\ &-\sum_{\{k_1,k_2\}}\sum_{\{k_3,k_4\}} A^*_{k_1',k_2}A_{k_3',k_4}\partial_{X(t)}\int_{-\infty}^{\infty}\psi_{k_1',k_2}(x)\mathcal{V}(x-X(t),y-Y(t))\psi_{k_3',k_4}(x)dxdy, \\ &M\frac{dv_y(t)}{dt} = \\ &-\sum_{\{k_1,k_2\}}\sum_{\{k_3,k_4\}} A^*_{k_1',k_2}A_{k_3',k_4}\partial_{Y(t)}\int_{-\infty}^{\infty}\psi_{k_1',k_2}(x)\mathcal{V}(x-X(t),y-Y(t))\psi_{k_3',k_4}(x)dxdy. \end{aligned} \tag{A4}$$

Here "*" is a conjugate of complex numbers. As a result, a closed system of $N+4$ first-order nonlinear differential equations is obtained.

The energy of the condensate interacting with the particle has the form:

$$\begin{aligned} E_C = &\sum_{\{k_1',k_2\}}\left|A_{k_1',k_2}\right|^2(k_1+1) \\ &+\sum_{\{k_1,k_2\}}\sum_{\{k_3,k_4\}} A^*_{k_1',k_2}A_{k_3',k_4}\int_{-\infty}^{\infty}\psi_{k_1',k_2}(x)\mathcal{V}(x-X(t),y-Y(t))\psi_{k_3',k_4}(x)dxdy, \end{aligned} \tag{A5}$$

and the total energy $E = E_C + M\left(v_x^2(t) + v_y^2(t)\right)/2$ is conserved.

The force interaction between the condensate ground state and parabolic potential is defined by

$$\begin{aligned} \mathbf{F}_c(t) &= -\frac{1}{2}\partial_{\langle\mathbf{r}(t)\rangle}\int_{-\infty}^{\infty} r^2|\psi(\mathbf{r}-\langle\mathbf{r}(t)\rangle,t)|^2 d^2r \\ &= -\frac{1}{2}\partial_{\langle\mathbf{r}(t)\rangle}\int_{-\infty}^{\infty}(\mathbf{r}'+\langle\mathbf{r}(t)\rangle)^2|\psi(\mathbf{r}',t)|^2 d^2r' \\ &= -\int_{-\infty}^{\infty}(\mathbf{r}'+\langle\mathbf{r}(t)\rangle)|\psi(\mathbf{r}',t)|^2 d^2r' = -\langle\mathbf{r}(t)\rangle. \end{aligned} \tag{A6}$$

Note

1 The truncated basis is considered as sufficient if increasing its size does not lead to the change in the numerically calculated results. For the systems considered here, sufficient basis contains $N = 21$ states and increasing it to 37 states produces no visible changes in the results obtained.

References

1. Landau, L.D. Electron motion in crystal lattices. *Phys. Z. Sowjet.* **1933**, *3*, 664.
2. Landau, L.; Pekar, S. Effective mass of a polaron. *Zh. Eksp. Teor. Fiz* **1948**, *18*, 419–423.
3. Feynman, R.P. Slow Electrons in a Polar Crystal. *Phys. Rev.* **1955**, *97*, 660–665. [CrossRef]
4. Zhang, F.C.; Rice, T.M. Effective Hamiltonian for the superconducting Cu oxides. *Phys. Rev. B* **1988**, *37*, 3759–3761. [CrossRef]

5. Konotop, V.V. Localized electron-phonon states originated by a three-wave interaction. *Phys. Rev. B* **1997**, *55*, R11926–R11928. [CrossRef]
6. Devreese, J.T. Fröhlich polarons from 0D to 3D: Concepts and recent developments*. *J. Physics Condens. Matter* **2007**, *19*, 255201. [CrossRef]
7. Semina, M.A.; Glazov, M.M.; Sherman, E. Interlayer Exciton–Polaron in Atomically Thin Semiconductors. *Annalen der Physik* **2020**, *532*, 2000339. [CrossRef]
8. Dalfovo, F.; Giorgini, S.; Pitaevskii, L.P.; Stringari, S. Theory of Bose-Einstein condensation in trapped gases. *Rev. Mod. Phys.* **1999**, *71*, 463–512. [CrossRef]
9. Leggett, A.J. Bose-Einstein condensation in the alkali gases: Some fundamental concepts. *Rev. Mod. Phys.* **2001**, *73*, 307–356. [CrossRef]
10. Cucchietti, F.M.; Timmermans, E. Strong-Coupling Polarons in Dilute Gas Bose-Einstein Condensates. *Phys. Rev. Lett.* **2006**, *96*, 210401. [CrossRef]
11. Shashi, A.; Grusdt, F.; Abanin, D.A.; Demler, E. Radio-frequency spectroscopy of polarons in ultracold Bose gases. *Phys. Rev. A* **2014**, *89*, 053617. [CrossRef]
12. Pastukhov, V. Polaron in the dilute critical Bose condensate. *J. Phys. Math. Theor.* **2018**, *51*, 195003. [CrossRef]
13. Khan, M.M.; Terças, H.; Mendonça, J.T.; Wehr, J.; Charalambous, C.; Lewenstein, M.; Garcia-March, M.A. Quantum dynamics of a Bose polaron in a *d*-dimensional Bose-Einstein condensate. *Phys. Rev. A* **2021**, *103*, 023303. [CrossRef]
14. Casteels, W.; Tempere, J.; Devreese, J.T. Polaronic properties of an impurity in a Bose-Einstein condensate in reduced dimensions. *Phys. Rev. A* **2012**, *86*, 043614. [CrossRef]
15. Abdullaev, F.K.; Salerno, M. Gap-Townes solitons and localized excitations in low-dimensional Bose-Einstein condensates in optical lattices. *Phys. Rev. A* **2005**, *72*, 033617. [CrossRef]
16. Schirotzek, A.; Wu, C.H.; Sommer, A.; Zwierlein, M.W. Observation of Fermi Polarons in a Tunable Fermi Liquid of Ultracold Atoms. *Phys. Rev. Lett.* **2009**, *102*, 230402. [CrossRef]
17. Sekino, Y.; Tajima, H.; Uchino, S. Mesoscopic spin transport between strongly interacting Fermi gases. *Phys. Rev. Res.* **2020**, *2*, 023152. [CrossRef]
18. Chevy, F.; Mora, C. Ultra-cold polarized Fermi gases. *Rep. Prog. Phys.* **2010**, *73*, 112401. [CrossRef]
19. Massignan, P.; Zaccanti, M.; Bruun, G.M. Polarons, dressed molecules and itinerant ferromagnetism in ultracold Fermi gases. *Rep. Prog. Phys.* **2014**, *77*, 034401. [CrossRef]
20. Koschorreck, M.; Pertot, D.; Vogt, E.; Fröhlich, B.; Feld, M.; Köhl, M. Attractive and repulsive Fermi polarons in two dimensions. *Nature* **2012**, *485*, 619–622. [CrossRef]
21. Prokof'ev, N.; Svistunov, B. Fermi-polaron problem: Diagrammatic Monte Carlo method for divergent sign-alternating series. *Phys. Rev. B* **2008**, *77*, 020408. [CrossRef]
22. Tempere, J.; Casteels, W.; Oberthaler, M.K.; Knoop, S.; Timmermans, E.; Devreese, J.T. Feynman path-integral treatment of the BEC-impurity polaron. *Phys. Rev. B* **2009**, *80*, 184504. [CrossRef]
23. Rath, S.P.; Schmidt, R. Field-theoretical study of the Bose polaron. *Phys. Rev. A* **2013**, *88*, 053632. [CrossRef]
24. Astrakharchik, G.E.; Pitaevskii, L.P. Motion of a heavy impurity through a Bose-Einstein condensate. *Phys. Rev. A* **2004**, *70*, 013608. [CrossRef]
25. Takahashi, J.; Imai, R.; Nakano, E.; Iida, K. Bose polaron in spherical trap potentials: Spatial structure and quantum depletion. *Phys. Rev. A* **2019**, *100*, 023624. [CrossRef]
26. Drescher, M.; Salmhofer, M.; Enss, T. Theory of a resonantly interacting impurity in a Bose-Einstein condensate. *Phys. Rev. Res.* **2020**, *2*, 032011. [CrossRef]
27. Boudjemâa, A. Self-localized state and solitons in a Bose-Einstein-condensate–impurity mixture at finite temperature. *Phys. Rev. A* **2014**, *90*, 013628. [CrossRef]
28. Mardonov, S.N.; Ahmedov, B.J.; Sherman, E.Y. Gravitating polarons in Bose–Einstein condensate: A contribution to the dark matter substance? *Eur. Phys. J. Plus* **2022**, *137*, 884. [CrossRef]
29. Catani, J.; Lamporesi, G.; Naik, D.; Gring, M.; Inguscio, M.; Minardi, F.; Kantian, A.; Giamarchi, T. Quantum dynamics of impurities in a one-dimensional Bose gas. *Phys. Rev. A* **2012**, *85*, 023623. [CrossRef]
30. Mardonov, S.N.; Sherman, E.Y. Coupled dynamics of polaron and Bose-Einstein condensate in a parabolic potential. *Phys. Scr.* **2020**, *96*, 035205. [CrossRef]
31. Penna, V.; Richaud, A. The phase-separation mechanism of a binary mixture in a ring trimer. *Sci. Rep.* **2018**, *8*, 10242. [CrossRef] [PubMed]
32. Mardonov, S.N. Collapse of quasi-two-dimensional symmetrized Dresselhaus spin-orbit coupled Bose–Einstein condensate. *Arab. J. Math.* **2022**, *11*, 43–47. [CrossRef]
33. Adhikari, S.K. Collapse of attractive Bose-Einstein condensed vortex states in a cylindrical trap. *Phys. Rev. E* **2001**, *65*, 016703. [CrossRef]
34. Mardonov, S.; Sherman, E.Y.; Muga, J.G.; Wang, H.W.; Ban, Y.; Chen, X. Collapse of spin-orbit-coupled Bose-Einstein condensates. *Phys. Rev. A* **2015**, *91*, 043604. [CrossRef]
35. Griffin, A.; Shukla, V.; Brachet, M.E.; Nazarenko, S. Magnus-force model for active particles trapped on superfluid vortices. *Phys. Rev. A* **2020**, *101*, 053601. [CrossRef]

36. Shukla, V.; Pandit, R.; Brachet, M. Particles and fields in superfluids: Insights from the two-dimensional Gross-Pitaevskii equation. *Phys. Rev. A* **2018**, *97*, 013627. [CrossRef]
37. Rønning, J.; Skaugen, A.; Hernández-García, E.; Lopez, C.; Angheluta, L. Classical analogies for the force acting on an impurity in a Bose–Einstein condensate. *New J. Phys.* **2020**, *22*, 073018. [CrossRef]
38. Lampo, A.; Charalambous, C.; García-March, M.A.; Lewenstein, M. Non-Markovian polaron dynamics in a trapped Bose-Einstein condensate. *Phys. Rev. A* **2018**, *98*, 063630. [CrossRef]
39. Mardonov, S.; Modugno, M.; Sherman, E.Y. Dynamics of a macroscopic spin qubit in spin–orbit coupled Bose–Einstein condensates. *J. Phys. B At. Mol. Opt. Phys.* **2015**, *48*, 115302. [CrossRef]
40. Pérez-García, V.M.; Michinel, H.; Cirac, J.I.; Lewenstein, M.; Zoller, P. Low Energy Excitations of a Bose-Einstein Condensate: A Time-Dependent Variational Analysis. *Phys. Rev. Lett.* **1996**, *77*, 5320–5323. [CrossRef] [PubMed]